

Sussex Research

Signatures of non-gaussianity in the isocurvature modes of primordial black hole dark matter

Sam Young, Christian Byrnes

Publication date

01-04-2015

Licence

This work is made available under the **Copyright not evaluated** licence and should only be used in accordance with that licence. For more information on the specific terms, consult the repository record for this item.

Citation for this work (American Psychological Association 7th edition)

Young, S., & Byrnes, C. (2015). *Signatures of non-gaussianity in the isocurvature modes of primordial black hole dark matter* (Version 1). University of Sussex. <https://hdl.handle.net/10779/uos.23416328.v1>

Published in

Journal of Cosmology and Astroparticle Physics

Link to external publisher version

<https://doi.org/10.1088/1475-7516/2015/04/034>

Copyright and reuse:

This work was downloaded from Sussex Research Open (SRO). This document is made available in line with publisher policy and may differ from the published version. Please cite the published version where possible. Copyright and all moral rights to the version of the paper presented here belong to the individual author(s) and/or other copyright owners unless otherwise stated. For more information on this work, SRO or to report an issue, you can contact the repository administrators at sro@sussex.ac.uk. Discover more of the University's research at <https://sussex.figshare.com/>

Young, Sam and Byrnes, Christian T

Signatures of non-gaussianity in the isocurvature modes of primordial black hole dark matter

Article (Unspecified)

Original citation:

Young, Sam and Byrnes, Christian T (2015) Signatures of non-gaussianity in the isocurvature modes of primordial black hole dark matter. *Journal of Cosmology and Astroparticle Physics*, 1504 (04). p. 34. ISSN 1475-7516

This version is available from Sussex Research Online: <http://sro.sussex.ac.uk/53944/>

This document is made available in accordance with publisher policies and may differ from the published version or from the version of record. If you wish to cite this item you are advised to consult the publisher's version. Please see the repository URL above for details on accessing the published version

Copyright and reuse:

Sussex Research Online is a digital repository of the research output of the University.

Copyright and all moral rights to the version of the paper presented here belong to the individual author(s) and/or other copyright owners. To the extent reasonable and practicable, the material made available in SRO has been checked for eligibility before being made available.

Copies of full text items generally can be reproduced, displayed or performed and given to third parties in any format or medium for personal research or study, educational, or not-for-profit purposes without prior permission or charge, provided that the authors, title and full bibliographic details are credited, a hyperlink and/or URL is given for the original metadata page and the content is not changed in any way.

Signatures of non-gaussianity in the isocurvature modes of primordial black hole dark matter

Sam Young¹, Christian T. Byrnes²

Department of Physics and Astronomy, Pevensey II Building, University of Sussex, BN1 9RH, UK

¹S.M.Young@sussex.ac.uk, ²C.Byrnes@sussex.ac.uk

May 6, 2015

Primordial black holes (PBHs) are black holes which may have formed very early on during the radiation dominated era in the early universe. We present here a method by which the large scale perturbations in the density of primordial black holes may be used to place tight constraints on non-gaussianity if PBHs account for dark matter (DM). The presence of local-type non-gaussianity is known to have a significant effect on the abundance of primordial black holes, and modal coupling from the observed CMB scale modes can significantly alter the number density of PBHs that form within different regions of the universe, which appear as DM isocurvature modes. Using the recent *Planck* constraints on isocurvature perturbations, we show that PBHs are excluded as DM candidates for even very small local-type non-gaussianity, $|f_{NL}| \approx 0.001$ and remarkably the constraint on g_{NL} is almost as strong. Even small non-gaussianity is excluded if DM is composed of PBHs. If local non-Gaussianity is ever detected on CMB scales, the constraints on the fraction of the universe collapsing into PBHs (which are massive enough to have not yet evaporated) will become much tighter.

Contents

1	Introduction	1
2	Calculating the abundance of PBHs	3
2.1	Calculating the abundance of PBHs in the presence of non-gaussianity	4
3	Modal coupling and the peak-background split	5
3.1	Quadratic non-gaussianity, f_{NL}	6
3.2	Cubic non-gaussianity, g_{NL}	7
4	The isocurvature modes of PBH DM on CMB scales	8
4.1	Isocurvature modes from f_{NL}	10
4.2	Isocurvature modes from g_{NL}	12
5	Further consideration of constraints from isocurvature modes	13
5.1	Isocurvature modes from f_{NL} and g_{NL}	13
5.2	Fractional primordial black hole DM	14
5.3	Intermediate modes	15
5.4	Higher Order terms	17
6	Summary	18
7	Acknowledgements	19
A	Full expression for δ_β from a g_{NL} term	19
B	Comparison with “Primordial black holes as biased tracers”	20

1 Introduction

Primordial black holes (PBHs) are black holes which theoretical arguments suggest might have formed from the direct gravitational collapse of large density perturbations very shortly after the end of inflation. PBHs may theoretically form with any mass, although their abundance is typically well constrained by observations. Whilst PBHs with mass lower than 10^{15}g would have evaporated by today (with the possible exception of Planck mass relics), more massive PBHs would still survive, and represent a viable dark matter (DM) candidate.

Many efforts have been made to observe PBHs, and whilst they have not yet been seen, this has led to many corresponding constraints on their abundance in different mass ranges [1]. The constraints typically assume that PBHs form at a single mass scale and are stated in terms of the mass fraction of the universe going into PBHs at the time of formation, β . There exists only a narrow window in which PBHs of a single mass could make up the entirety of DM, with other scales being excluded by observations. It is noted that there has been a recent claim that the tidal capture of PBHs by neutron stars could be used to exclude the remaining window (apart from Planck mass remnants) [2], but this has been refuted in [3, 4]. The results presented here can also be applied if DM is composed of smaller PBHs which have all but evaporated by today leaving Planck mass remnants which may make up DM [5]. Whilst this mass range is not explicitly considered, it is certainly not ruled out by observations, and the results presented here are almost independent of the PBH mass.

In order for a significant number of PBHs to form, the power spectrum on small scales needs to be significantly larger than observed in the CMB - of order 10^{-2} in the case of gaussian perturbations. This is possible in many models of inflation, including the running mass model [6], axion inflation [7], a waterfall transition during hybrid inflation [8, 9, 10], from passive density fluctuations [11], or in inflationary models with small field excursions but which are tuned to produce a large tensor-to-scalar ratio on large scales [12]. See also [13, 14, 15], and a summary of various models which can produce PBHs is presented in [16]. Alternatively, the constraint on the formation criteria can be relaxed during a phase transition in the early universe, causing PBHs to form preferentially at that mass scale [17] - although such an effect will not be considered here.

PBHs have traditionally been used to investigate the early universe by placing a constraint on the small scale power spectrum from the corresponding constraint on their abundance [18, 19, 20]. In this paper, large scale fluctuations in the PBH density caused by local-type non-gaussianity are considered. If DM is composed entirely, or partially, of PBHs, these perturbations will be seen as isocurvature modes in cold dark matter (CDM) - upon which there are tight constraints from the recent *Planck* data release [21].

The isocurvature perturbations are formed in a highly non-linear manner in this model. PBHs form shortly after horizon reentry during radiation domination, with an energy density exponentially sensitive to the amplitude of the power spectrum. Observational constraints imply that at most one region in a million collapsed into a PBH so the large scale radiation density is almost unaffected, but if PBHs form DM then the amplitude of the DM perturbation is extremely sensitive to the modal coupling. Using this mechanism, CDM (with zero pressure) is formed in a universe which could have previously have been made up entirely of radiation and hence had no isocurvature perturbation prior to PBH formation. Such an effect is impossible within linear perturbation theory [22].

In a previous paper, the peak-background split was used to investigate the effect of modal coupling on the constraints which can be placed on the small scale power spectrum [23]. In this paper we use the same mechanism to investigate the extent to which modal coupling produces CDM isocurvature modes and discuss the implications of such an effect. Even if the initial conditions are adiabatic, which has been shown to be the case in single-field inflation, if there is modal coupling then the conversion of radiation into CDM (by collapse into PBHs) can have different efficiencies in different regions of the universe, which introduces isocurvature modes in the CDM after inflation has ended.

Even single-field inflation generates a small value of f_{NL} with magnitude comparable to the spectral index [24] - which apparently could therefore rule out single-field inflation as a mechanism to create PBH DM. However, it has been argued that this is a result of gauge choice [25, 26], and that for our purposes the effective $f_{NL} = 0$ in single-field inflation. It is therefore assumed in this paper that f_{NL} can be arbitrarily close to zero.

Throughout, we will assume f_{NL} to be scale invariant whilst the power spectrum becomes several orders of magnitude larger at small scales - which is likely to be unrealistic given a specific model. However, this is a conservative approach, because if $|f_{NL}|$ were to become larger at some small scale, it would not weaken the constraints derived here, but would be likely to strengthen them. Even if the bispectrum was exactly zero when all three modes have sub CMB scales, the modal coupling between the CMB and PBH scales would still effect the amplitude of the power spectrum on PBH scales and the constraints which we derive would not be significantly weakened. In such a case, the perturbations within a region smaller than we can probe on the CMB would be Gaussian, but the variance would vary between different patches, in a way completely correlated to the long wavelength perturbation.

Shortly prior to the release of this paper, Tada and Yokoyama [27] released a paper discussing

a similar effect and the use of PBHs as biased tracers. We confirm their results and extend the calculation to account for the non-gaussianity parameter g_{NL} as well as f_{NL} , the effect of intermediate modes (between the CMB- and PBH-scales), and make use of the more recent results from the *Planck* 2015 data release. Because all surviving PBHs necessarily behave as at least a subdominant DM component today, we also show how the allowed fraction of PBHs can be constrained more tightly than previously realised, under the presence of even small non-Gaussianity.

The layout of this paper is as follows: in section 2, the calculation of the PBH abundance, in both the gaussian and non-gaussian case, is reviewed. In section 3, modal coupling and how the peak-background split may be used to investigate its effects on PBH abundance is discussed. In section 4, the calculation is applied to the formation of CDM isocurvature modes and place constraints on the non-gaussianity parameters in the case of PBH DM, and the calculation is extended to include simultaneous f_{NL} and g_{NL} , intermediate modes, and the case where PBHs only make up a portion of the DM. We conclude with a summary of our arguments in section 6.

2 Calculating the abundance of PBHs

The abundance of PBHs is normally stated in terms of β : the energy fraction of the universe going into PBHs at the time of formation. The standard calculation used in the literature uses a Press-Schechter approach, although it has been shown that, for a gaussian distribution, this matches well when the theory of peaks is used. It has been argued that the density contrast, rather than the curvature perturbation, should be used - although an approximation using the curvature perturbation works very well if care is taken to exclude super-horizon modes from the calculation, and this simplifies the calculation greatly. In this section, we will briefly review the calculation, as well as the main sources of error, for both gaussian and non-gaussian cases.

When a perturbation reenters the horizon, if its amplitude exceeds a certain threshold, or critical, value, then gravitational forces will overcome pressure forces and the region will collapse to form a primordial black hole. There has been extensive research to calculate the threshold value [28, 29, 30, 31, 32, 33], which is typically stated in terms of the density contrast. The critical value of the density perturbation is believed to be $\delta_c \approx 0.45$. However, in this paper the curvature perturbation is used, and the corresponding critical value is $\zeta_c \approx 1$ - within the range found by [34], and is consistent with using the density contrast [35].

The main source of uncertainty in the critical value is due to the unknown shape of primordial perturbations - and this is the largest source of error in the calculation of the abundance. However, whilst the effect on the calculated value of the abundance is large, the effect of this uncertainty on derived parameters is relatively small. For example, an error of $\mathcal{O}10\%$ in the threshold value results in an error of several orders of magnitude in the calculated β but only an error of $\mathcal{O}10\%$ in the constraint on the power spectrum [36, 37]. In this paper, because our results depend only on the relative abundance of PBHs in different regions of the universe, the conclusions are not sensitive to small changes in the threshold value.

Using a Press-Schechter approach, the mass fraction of the universe going into PBHs at the time of formation is given by integrating over the probability density function (PDF),

$$\beta = \int_{\zeta_c}^{\infty} P(\zeta) d\zeta. \quad (1)$$

In the case of a gaussian distribution, the probability density function is

$$P(\zeta) = \frac{1}{\sqrt{2\pi\sigma^2}} \exp\left(-\frac{\zeta^2}{2\sigma^2}\right), \quad (2)$$

Where σ^2 is the variance of perturbation amplitude at the PBH forming scale. β can therefore be written in terms of the complimentary error,

$$\beta = \text{erfc}\left(\frac{\zeta_c}{\sqrt{2\sigma^2}}\right). \quad (3)$$

Expanding using the large-x limit of $\text{erfc}(x)$, gives

$$\beta \approx \sqrt{\frac{2\sigma^2}{\pi\zeta_c^2}} \exp\left(-\frac{\zeta_c^2}{2\sigma^2}\right). \quad (4)$$

This is valid only if the distribution is gaussian, and because PBHs form in the extreme positive tail of the PDF, their abundance is very sensitive to any non-gaussianity, which we discuss below.

2.1 Calculating the abundance of PBHs in the presence of non-gaussianity

In the local model of non-gaussianity, the curvature perturbation is given by

$$\zeta = \zeta_G + \frac{3}{5}f_{NL}(\zeta_G^2 - \sigma^2) + \frac{9}{25}g_{NL}\zeta_G^3 + \dots = h(\zeta_G), \quad (5)$$

where σ^2 is the variance of the gaussian variable ζ_G , and is subtracted to ensure the expectation value of ζ is zero.

The calculation of the abundance of PBHs is most easily performed by calculating the values of ζ_G which correspond the critical value, ζ_c , and integrating over the corresponding regions of the gaussian PDF of ζ_G - the reader is directed to [36, 37] for a full derivation. For example, let us consider the case where g_{NL} and higher order terms are zero:

$$\zeta = \zeta_G + \frac{3}{5}f_{NL}(\zeta_G^2 - \sigma^2) = h(\zeta_G). \quad (6)$$

$h^{-1}(\zeta_c)$ therefore has two solutions, given by

$$h_{c\pm}^{-1} = h_{\pm}^{-1}(\zeta_c) = \frac{-5 \pm \sqrt{25 + 60\zeta_c f_{NL} + 36\zeta_c^2 f_{NL}^2 \sigma^2}}{6f_{NL}}. \quad (7)$$

For positive f_{NL}

$$\beta = \sqrt{\frac{2}{\pi\sigma^2}} \left(\int_{h_{c+}^{-1}}^{\infty} \exp\left(-\frac{\zeta_G^2}{2\sigma^2}\right) d\zeta_G + \int_{-\infty}^{h_{c-}^{-1}} \exp\left(-\frac{\zeta_G^2}{2\sigma^2}\right) d\zeta_G \right), \quad (8)$$

and for negative f_{NL}

$$\begin{aligned} \beta &= \sqrt{\frac{2}{\pi\sigma^2}} \int_{h_{c+}^{-1}}^{h_{c-}^{-1}} \exp\left(-\frac{\zeta_G^2}{2\sigma^2}\right) d\zeta_G \\ &= \sqrt{\frac{2}{\pi\sigma^2}} \left(\int_{h_{c+}^{-1}}^{\infty} \exp\left(-\frac{\zeta_G^2}{2\sigma^2}\right) d\zeta_G - \int_{h_{c-}^{-1}}^{\infty} \exp\left(-\frac{\zeta_G^2}{2\sigma^2}\right) d\zeta_G \right). \end{aligned} \quad (9)$$

Furthermore, if we make the assumption that f_{NL} is small, $f_{NL} \ll 1$, which we will show is justified in the case that DM is composed of PBHs (and is further verified by the findings of [27]), the above expressions can be simplified further. In the expression of β for positive and negative f_{NL} , the first term inside the brackets dominates, and β can be written in terms of one complimentary error function,

$$\begin{aligned}\beta &= \sqrt{\frac{2}{\pi\sigma^2}} \int_{h_{c+}^{-1}}^{\infty} \exp\left(-\frac{\zeta_G^2}{2\sigma^2}\right) d\zeta_G \\ &= \text{erfc}\left(\frac{h_{c+}^{-1}}{\sqrt{2}\sigma}\right) \\ &\approx \sqrt{\frac{2\sigma^2}{\pi(h_{c+}^{-1})^2}} \exp\left(-\frac{(h_{c+}^{-1})^2}{2\sigma^2}\right).\end{aligned}\tag{10}$$

Deriving an analytic expression as shown here is not a necessary step, but it is a useful approximation, and we will later use this result to derive an analytic expression for bias factor and amplitude of isocurvature modes in the PBH density.

Although it is not shown here, the same calculation can be performed for the local model of non-gaussianity containing g_{NL} - the interested reader is again directed to [36, 37] for a full discussion of the calculation. In the case where only a cubic and linear term are considered

$$\zeta = \zeta_G + \frac{9}{25}g_{NL}\zeta_G^3 = h(\zeta_G),\tag{11}$$

then $h^{-1}(\zeta_c)$ has up to three possible solutions, depending on the value of g_{NL} and ζ_c . However, assuming that g_{NL} is small, $g_{NL} \ll 1$, which again will be shown later, the expression is dominated by one erfc function as in equation (10), with a different expression for $h^{-1}(\zeta_c)$. To first order in g_{NL}

$$h_c^{-1} = \zeta_c - \frac{9\zeta_c^3 g_{NL}}{25}.\tag{12}$$

3 Modal coupling and the peak-background split

It has previously been shown [35] that curvature perturbation modes which are a long way outside the horizon at the time of PBH formation have little effect on whether a PBH forms. This is due to the suppression of large scale density modes by a factor k^2 relative to the curvature perturbation. In radiation domination:

$$\delta(t, k) = \frac{2(1+\omega)}{5+3\omega} \left(\frac{k}{aH}\right)^2 \zeta(k) = \frac{4}{9} \left(\frac{k}{aH}\right)^2 \zeta(k),\tag{13}$$

where $\omega = 1/3$ is the equation of state, and $(aH)^{-1}$ is the horizon scale at the time of PBH formation. However, long wavelength modes can have an indirect effect on the abundance of PBHs, β , due to modal coupling from non-gaussianity. A long wavelength mode can affect both the amplitude and distribution of the small scale perturbations which may form PBHs. In figure 1, we show how the coupling of long- and short-wavelength modes can affect the number of PBHs forming in different regions of the universe. At the peak of the long wavelength mode, the amplitude of the small scale mode is increased, forming more PBHs, whilst the opposite occurs at the trough.

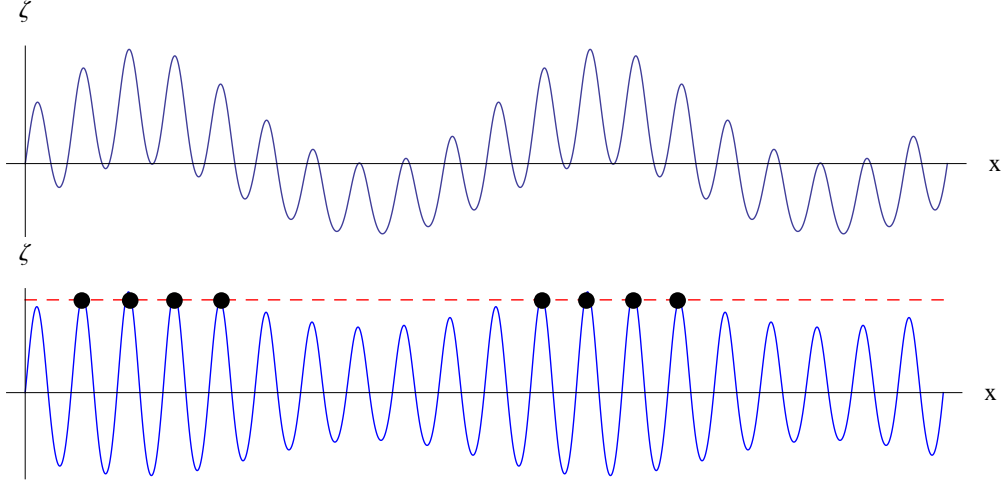


Figure 1: The top plot shows an example of a universe containing only two modes. As an example of modal coupling, the amplitude of the short wavelength mode is a function of the long wavelength mode - the amplitude of the short-wavelength mode is larger at the peak of the long-wavelength mode. At the time when short-wavelength mode enters the horizon, and PBHs at that scale form, the long-wavelength mode is not yet visible and will not affect whether a PBH forms or not. The bottom plot shows the same universe, but with the long wavelength mode subtracted, enabling ζ to be used as a formation criterion for PBHs. The dashed red line shows the formation threshold for PBHs - regions where the curvature perturbation is greater than the formation threshold will collapse to form a PBH. The black circles represent areas which will collapse to form a PBH. It can be seen that a relatively small change in the amplitude of the small scale mode can have a large impact on the number of PBHs forming in a region.

How modal coupling can affect the constraints on the power spectrum at small scales from PBHs has been investigated [23], although it was assumed that all the modes involved were sub-CMB and potentially had a large amplitude. In this paper, we will go beyond previous work and study the case where the large-scale modes are observable in the CMB and hence very small. Despite their small amplitude, we show that these perturbations have a remarkably large effect on observations. In this section, we will briefly review the calculation using the peak-background split to investigate modal coupling due to the local non-gaussianity parameters f_{NL} and g_{NL} , and in the following section, apply this to the abundance of PBHs and the creation of isocurvature modes.

3.1 Quadratic non-gaussianity, f_{NL}

We will take the model of local non-gaussianity, in terms of the curvature perturbation ζ , to be described by

$$\zeta = \zeta_G + \frac{3}{5}f_{NL}(\zeta_G^2 - \sigma^2) = h(\zeta_G), \quad (14)$$

where ζ_G is a gaussian variable. It is necessary to subtract $\sigma^2 = \langle \zeta_G^2 \rangle$ so that the background (average) value of ζ remains zero. We will now employ the peak-background split, and write the gaussian component as the sum of a long-(background) and short-(peak) wavelength component,

$$\zeta_G = \zeta_l + \zeta_s. \quad (15)$$

Equation (14) then becomes:

$$\zeta = (\zeta_l + \zeta_s) + \frac{3}{5}f_{NL} \left((\zeta_l + \zeta_s)^2 - \langle (\zeta_l + \zeta_s)^2 \rangle \right). \quad (16)$$

However, terms which depend only on the long-wavelength mode do not affect PBH formation, and should not be considered when determining the abundance of PBHs. We therefore subtract those terms, leaving:

$$\zeta = \left(1 + \frac{6}{5}f_{NL}\zeta_l \right) \zeta_s + \frac{3}{5}(\zeta_s^2 - \sigma_s^2). \quad (17)$$

We can now rewrite the expression in terms of new variables, $\tilde{\zeta}_G$, $\tilde{\sigma}$ and \tilde{f}_{NL} , and calculate the abundance of PBHs β as described in section 2, as a function of the long wavelength mode, ζ_l .

$$\begin{aligned} \tilde{\zeta}_G &= \left(1 + \frac{6}{5}f_{NL}\zeta_l \right) \zeta_s, \\ \tilde{\sigma} &= \left(1 + \frac{6}{5}f_{NL}\zeta_l \right) \sigma_s, \\ \tilde{f}_{NL} &= \left(1 + \frac{6}{5}f_{NL}\zeta_l \right)^{-2} f_{NL}. \end{aligned} \quad (18)$$

Equation (17) can then be written in a form analogous to equation (14),

$$\zeta = \tilde{\zeta}_G + \frac{3}{5}\tilde{f}_{NL}(\tilde{\zeta}_G^2 - \tilde{\sigma}^2) = \tilde{h}(\tilde{\zeta}_G). \quad (19)$$

Therefore, both the amplitude and distribution of the small-scale perturbations are affected. In order to calculate the abundance of PBHs, the variables in equation (18) can then be inserted into equation (10).

3.2 Cubic non-gaussianity, g_{NL}

Here, we will follow the same steps as for f_{NL} , to show how the presence of a cubic term causes modal coupling. For this section, we will assume $f_{NL} = 0$, and ζ to be given by

$$\zeta = \zeta_G + \frac{9}{25}g_{NL}\zeta_G^3. \quad (20)$$

Again, using the peak-background split, one obtains:

$$\zeta = \left(1 + \frac{27}{25}g_{NL}\zeta_l^2 \right) \zeta_s + \left(\frac{27}{25}g_{NL}\zeta_l \right) \zeta_s^2 + \left(\frac{9}{25}g_{NL} \right) \zeta_s^3 + \mathcal{O}(\zeta_l), \quad (21)$$

where again, the terms dependant only on ζ_l are neglected because they don't have a significant effect on PBH formation. The above expression can then be rewritten in terms of new variables $\tilde{\zeta}_G$, $\tilde{\sigma}$, \tilde{f}_{NL} and \tilde{g}_{NL} , given by

$$\begin{aligned} \tilde{\zeta}_G &= \left(1 + \frac{27}{25}g_{NL}\zeta_l^2 \right) \zeta_s, \\ \tilde{\sigma} &= \left(1 + \frac{27}{25}g_{NL}\zeta_l^2 \right) \sigma_s, \\ \tilde{f}_{NL} &= \left(\frac{9}{25}g_{NL}\zeta_l \right) \left(1 + \frac{27}{25}g_{NL}\zeta_l^2 \right)^{-2}, \\ \tilde{g}_{NL} &= g_{NL} \left(1 + \frac{27}{25}g_{NL}\zeta_l^2 \right)^{-3}. \end{aligned} \quad (22)$$

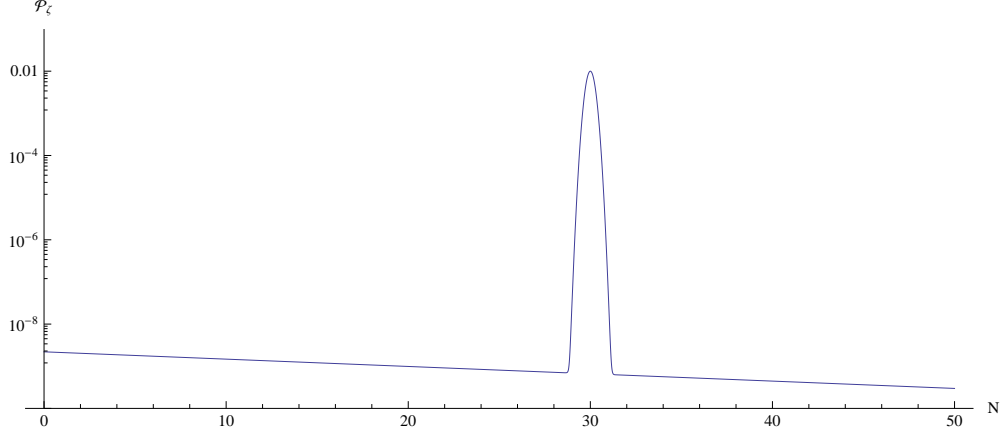


Figure 2: An example of a power spectrum containing a narrow peak. N represents number of e-folds, with smaller scales represented by larger N . The power spectrum is small on most scales with a spectral index of $n_S = 0.96$, compatible with observations of the cosmic microwave background (CMB) and large scale structure (LSS). The narrow peak in the power spectrum corresponds to the scale at which will PBHs form.

Equation (20) can then be rewritten as

$$\zeta = \tilde{\zeta}_G + \frac{3}{5}f_{NL} \left(\tilde{\zeta}_G^2 - \tilde{\sigma}^2 \right) + \frac{9}{25}\tilde{g}_{NL}\tilde{\zeta}_G^3. \quad (23)$$

An expression for the abundance of PBHs in a given region of the universe, $\tilde{\beta}$, can then be derived as shown in section 2.

In this section, it has been shown that long wavelength modes can affect the amplitude of local small scale perturbations and the non-gaussianity parameters, and in the next section the effect of this on the abundance of PBHs within a given region will be discussed.

4 The isocurvature modes of PBH DM on CMB scales

The abundance of PBHs in a region of the universe can be affected significantly by large-scale curvature perturbation modes in different regions of the universe. If PBHs make up DM, then these differences in the abundance of PBHs will appear as fluctuations in the density of DM. In the presence of local-type non-gaussianity, the fluctuations in the DM can be significantly greater than the curvature perturbations responsible for producing them - and tight constraints can therefore be placed on the non-gaussianity parameters if this is the case from the isocurvature constraints from *Planck*.

We will define the difference in the abundance of PBHs at the time of formation, δ_β , as

$$\delta_\beta = \frac{\beta - \bar{\beta}}{\bar{\beta}}, \quad (24)$$

where β and $\bar{\beta}$ are the perturbed and background values of the PBH abundance at the time of formation respectively. If the large-scale curvature perturbation ζ is small, it can be related to δ_β by a constant factor b (referred to the scale dependant bias in [27]),

$$\delta_\beta = b\zeta_l, \quad (25)$$

where b is a function of the non-gaussianity parameters, the variance of the small-scale perturbations and the critical value for PBH formation ζ_c . The factor b therefore parameterises the bias of PBHs to form in the presence of large-scale curvature perturbations.

In this section, we will consider the case where the power spectrum is very small on all scales, except for a narrow region where there is a sharp spike - which is responsible for the production of PBHs of a mass corresponding to this scale¹. An example of such a power spectrum is given in figure 2. We therefore ignore in this section the presence of perturbations of intermediate scales, but extend the calculation in the following section to account for when there is a broad peak in the power spectrum.

The abundance of PBHs at a later time on a comoving slicing will be affected by difference in their density at the time of formation, as well as by the difference in expansion since the time of formation - in denser regions of the universe, inflation ends and PBHs form slightly later, so even if the PBH density is constant at the time of formation, the density will not be constant. To first order in ζ , the density of PBHs can be expressed as

$$\Omega_{PBH} = (1 + b\zeta + 3\zeta) \bar{\Omega}_{PBH}, \quad (26)$$

where the 3ζ term is simply the adiabatic mode expected from the expansion of the universe, and $\bar{\Omega}_{PBH}$ is the background density of PBHs. The $b\zeta$ term therefore represents a deviation from the expected amplitude of the mode if it was purely adiabatic - it is an isocurvature mode, which will either be fully correlated, or fully anti-correlated depending on the sign of f_{NL} . If PBHs make up a significant fraction of the DM content of the universe, the constraints on isocurvature modes from *Planck* can then be used to constrain b - and therefore constrain the non-gaussianity parameters². For simplicity in this paper, except section 5.2, we will assume that DM is entirely composed of PBHs, and calculate corresponding constraints on the non-gaussianity parameters f_{NL} and g_{NL} . On CMB scales, the constraints from *Planck* on isocurvature modes can be used [21]

$$100\beta_{iso} = \begin{cases} 0.13 & , \text{fully correlated} \\ 0.08 & , \text{fully anti-correlated,} \end{cases} \quad (27)$$

where

$$\beta_{iso} = \frac{\mathcal{P}_{iso}}{\mathcal{P}_{iso} + \mathcal{P}_{\zeta}}. \quad (28)$$

The fully correlated modes correspond to positive b , whilst fully anti-correlated corresponds to negative b (and positive/negative f_{NL} and g_{NL} respectively). The isocurvature power spectrum is related to the curvature perturbation power spectrum as

$$\mathcal{P}_{iso} = b^2 \mathcal{P}_{\zeta}, \quad (29)$$

and we therefore obtain constraints on b as

$$-0.028 < b < 0.036. \quad (30)$$

This result will now be used to derive a result on the non-gaussianity parameters.

¹The mass of a PBH is roughly equal to the horizon mass at the time of formation. See [35] for further discussion.

²Note that the reverse is also true - for a given value of the non-gaussianity parameters, an upper limit can be placed on the amount of DM which is made of PBHs

4.1 Isocurvature modes from f_{NL}

In section 2, an expression for the abundance of PBHs at the time of formation β , was derived in terms of the non-gaussianity parameter f_{NL} , the variance of the gaussian component³ σ^2 , and the critical value for collapse ζ_c - equation (10), with h^{-1} given by equation (7). However, this calculation assumes there is no coupling to large scale modes (and is equivalent to the background value, $\bar{\beta}$, if large-scale perturbations are small - as is the case here). In section 3 it was shown how to account for the presence of a large scale modes - namely, by using the transformed variables \tilde{f}_{NL} and $\tilde{\sigma}$ instead, given by equation (18) - which calculates the perturbed abundance β .

By combining equations (7), (8), (9), (18) and (24), it is possible to derive an expression for δ_β in terms of f_{NL} , σ_s (where the s subscript has been adopted to denote the small PBH scale), and the critical value ζ_c . Expanding the expression to first order in ζ gives the result

$$\delta_\beta = \frac{25 + 30\zeta_c f_{NL} + 36f_{NL}^2 \sigma_{st}^2 - 5\sqrt{25 + 60\zeta_c f_{NL} + 36f_{NL}^2 \sigma_s^2}}{3f_{NL} \sigma_s^2 \sqrt{25 + 60\zeta_c f_{NL} + 36f_{NL}^2 \sigma_s^2}} \zeta, \quad (32)$$

and therefore b is given by

$$b = \frac{25 + 30\zeta_c f_{NL} + 36f_{NL}^2 \sigma_{st}^2 - 5\sqrt{25 + 60\zeta_c f_{NL} + 36f_{NL}^2 \sigma_s^2}}{3f_{NL} \sigma_s^2 \sqrt{25 + 60\zeta_c f_{NL} + 36f_{NL}^2 \sigma_s^2}}, \quad (33)$$

or to first order in f_{NL}

$$b = \frac{6}{5} \left(1 + \frac{\zeta_c^2}{\sigma_s^2} \right) f_{NL}. \quad (34)$$

As expected, a positive f_{NL} , which boosts the power spectrum on small scales in areas of higher density, produces a positive bias, and fully correlated isocurvature modes in PBH DM⁴. Negative f_{NL} has the opposite effect, and produces fully anti-correlated isocurvature modes.

In order to investigate the constraints on the non-gaussianity parameters, it is necessary to estimate values for the other parameters involved, and how these would affect the constraints. The variance of the small scale perturbations and the critical value.

- First, ζ_c is considered: there is significant error in the exact value of the threshold value, due to uncertainty in the shape of the primordial perturbation which collapse to form PBHs. Most recent simulations have calculated the critical value in terms of the density contrast, finding $\delta_c \approx 0.4$. This is consistent with the calculation here if the critical value of the curvature perturbation is related by a factor $\frac{4}{9}$, meaning $\zeta_c \approx 1$, which is consistent with the range of values found in figure [34]. Figure 3 shows how the factor b depends on the critical value for different values of f_{NL} .

³ σ is related to the power spectrum as follows [38]

$$\mathcal{P}_\zeta = \sigma^2 + \left(\frac{3}{5}\right)^2 (4f_{NL}^2 + 6g_{NL}) \sigma^4 \ln(kL) + \left(\frac{3}{5}\right)^4 (27g_{NL}^2) \sigma^6 \ln(kL)^2, \quad (31)$$

where the higher order terms from g_{NL} have also been included, and $\ln(kL)$ is a factor of around unity. Note that, since the non-gaussianity parameters are found to be very small, the higher order terms will not have a significant impact, and to a good approximation $\mathcal{P}_\zeta = \sigma^2$.

⁴The second expression for b corresponds to equation (14) in [27]. The more complicated expression, equation (33), is because a gaussian distribution on small scales has not been assumed. The differences between the 2 calculations are discussed in Appendix B.

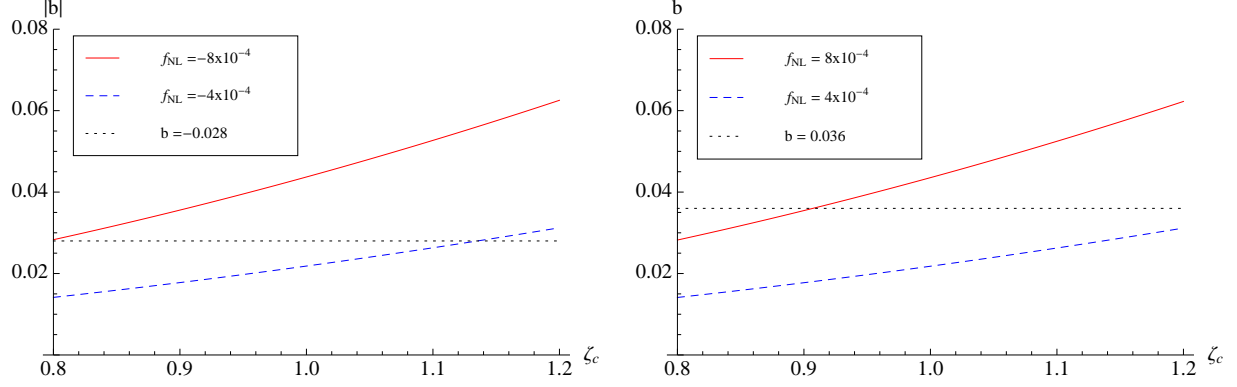


Figure 3: The plots above show the effects of a different threshold ζ_c on the PBH bias b arising from an f_{NL} term. A larger value of ζ_c suggests a larger bias factor. The left plot shows the effect for negative f_{NL} and the right plot for positive f_{NL} . The dotted black lines represent the constraints on b from the constraints on isocurvature modes from *Planck*. $|f_{NL}| = 8 \times 10^{-4}$ is typically excluded whilst $|f_{NL}| = 4 \times 10^{-4}$ is typically allowed. To generate these plots the value $\sigma = 0.15$ has been used.

- To calculate σ_s , it is necessary to first calculate the value of β for which PBHs are otherwise unconstrained by observations and could be DM. The range of mass scales in which PBHs can form a significant fraction of DM is roughly $10^{17}\text{g} < M_{PBH} < 10^{24}\text{g}$ [1]. The constraint on β from the abundance of DM in this range are given by [19]

$$\beta < 2 \times 10^{-19} \left(\frac{M_{PBH}}{f_M 5 \times 10^{14}\text{g}} \right)^{1/2}, \quad (35)$$

where f_M is the fraction of the horizon mass which ends up inside the PBH⁵, and M_{PBH} is the mass of the PBH. Assuming DM to be made up entirely of PBHs of a single mass scale within this range, β can therefore range from $\beta < 10^{-16}$ to $\beta < 10^{-11}$. Assuming the most optimistic and pessimistic values for β and ζ_c , σ_s is calculated to lie in the range $0.1 < \sigma_s < 0.2$ for close to gaussian perturbations [36]. Figure 4 displays how b changes with σ_s .

Smaller values of the variance of the small scale perturbations, σ_s^2 , would lead to tighter constraints on f_{NL} , whilst a smaller critical value ζ_c leads to tighter constraints on f_{NL} . Because a larger value of ζ_c implies a larger value of σ_s , these effects virtually cancel out - and the results presented below are therefore not sensitive to uncertainty in ζ_c .

Assuming PBH form at a single mass scale, the weakest constraint on f_{NL} comes from considering the mass of the largest PBHs which could make up DM, which is taken to be $M_{PBH} = 10^{25}\text{g}$, for which $\beta \approx 10^{-14}$. If DM is made entirely of PBHs, the constraints on f_{NL} are therefore

$$-4 \times 10^{-4} < f_{NL} < 5 \times 10^{-4}. \quad (36)$$

The results are not significantly different for PBHs of different mass. For example, for $M_{PBH} = 10^{20}\text{g}$ the constraints on f_{NL} are

$$-3 \times 10^{-4} < f_{NL} < 4 \times 10^{-4}. \quad (37)$$

⁵ f_M is a factor of order unity, which is neglected as it has very little effect on the calculated value of σ_s .

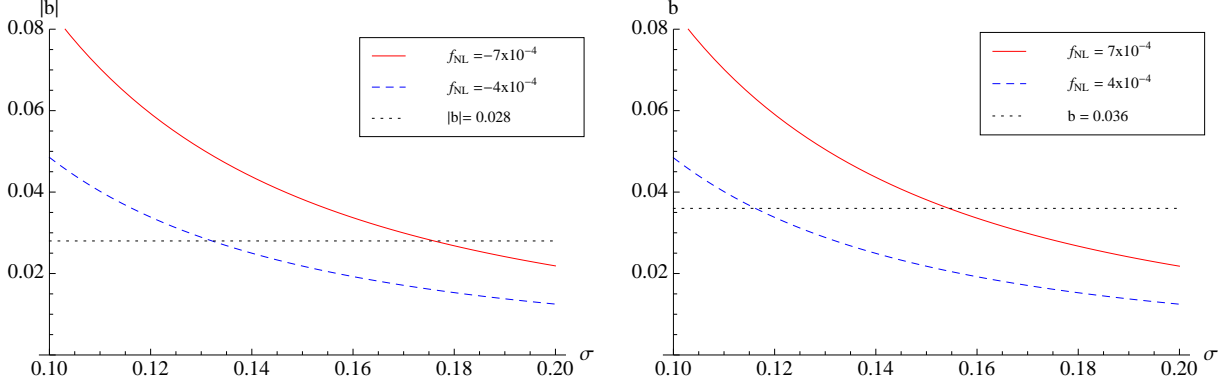


Figure 4: The effects of a different σ on the PBH bias b arising from an f_{NL} term are investigated. A larger value of σ suggests a smaller bias factor. The left plot shows the effect for negative f_{NL} and the right plot for positive f_{NL} . The dotted black lines represent the constraints on b from the constraints on isocurvature modes from *Planck*. $|f_{NL}| = 7 \times 10^{-4}$ is typically excluded whilst $|f_{NL}| = 4 \times 10^{-4}$ is typically allowed. To generate these plots the value $\zeta_c = 1$ has been used.

4.2 Isocurvature modes from g_{NL}

In addition to f_{NL} , it is interesting to consider isocurvature modes arising from g_{NL} and place constraints, or whether the effects of modal coupling from g_{NL} could cancel the effects from f_{NL} . The effect of higher order terms are beyond the scope of this paper.

The same derivation can be followed as that for f_{NL} , leading to an expression for b to first order in g_{NL}

$$b = -\frac{27(\sigma_s^2 - \zeta_c^2)(\sigma_s^2 + \zeta_c^2)}{25\sigma_s^2\zeta_c}g_{NL}. \quad (38)$$

Again, as expected, positive g_{NL} corresponds to fully correlated isocurvature modes, and negative g_{NL} corresponds to fully anti-correlated isocurvature modes. The PBH bias factor b is again a function of the non-gaussianity parameter g_{NL} , the variance of the small scale perturbations σ_s^2 , and the formation threshold ζ_c . The dependance of b on ζ_c and σ_s is shown in figures 5 and 6 respectively.

We see again that smaller values of σ_s would lead to tighter constraints on g_{NL} , whilst a smaller ζ_c leads to tighter constraints on g_{NL} . However, unlike the case with f_{NL} , the constraint which can be placed on g_{NL} depends on the value of ζ_c , although only by a factor of $\mathcal{O}(10\%)$. The results presented below are the weakest constraints, corresponding to a low formation threshold, for PBHs of mass 10^{25}g

$$-6 \times 10^{-4} < g_{NL} < 7 \times 10^{-4}. \quad (39)$$

Notice that these constraints are very comparable to those on f_{NL} , see (37). The f_{NL} term has an effect of $\mathcal{O}(10^{-5})$ on the small-scale power spectrum, whilst the g_{NL} term only has an effect of $\mathcal{O}(10^{-10})$, and therefore, naively, the constraints on g_{NL} would be expected to be roughly 5 orders of magnitude weaker than f_{NL} . However, a g_{NL} term also has an effect on the small scale \tilde{f}_{NL} , as seen in equation (22), of $\mathcal{O}(10^{-5})$, and because the abundance of PBHs is extremely sensitive to non-gaussianity, this causes significant isocurvature modes in the PBH DM. In the case where $\zeta_l = 10^{-5}$ and $g_{NL} = 10^{-3}$, then $\tilde{f}_{NL} \approx 10^{-8}$. Such a small \tilde{f}_{NL} nonetheless creates a perturbation in the PBH density of $\mathcal{O}(10^{-6})$, which represents an isocurvature mode of around 10% of ζ - which is excluded by *Planck*. Because the abundance of PBHs β is sensitive to higher order non-gaussianity

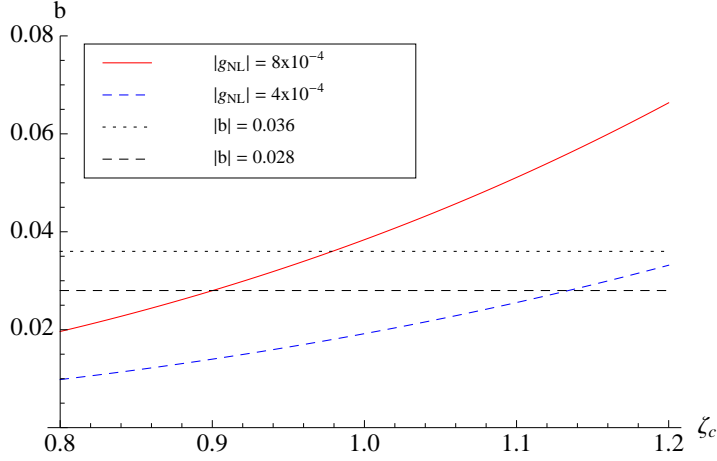


Figure 5: The plots above show the effects of a different threshold ζ_c on the PBH bias b arising from a g_{NL} term. A larger value of ζ_c suggests a larger bias factor. As the expression for b , equation (38), is anti-symmetric under a change of sign of g_{NL} , the results for negative and positive g_{NL} are shown on one plot - but with different constraints on the amplitude of $|b|$, represented by the dotted black lines. $|g_{NL}| = 8 \times 10^{-4}$ is typically excluded whilst $|g_{NL}| = 4 \times 10^{-4}$ is typically allowed. To generate these plots the value $\sigma = 0.15$ has been used.

parameters [37], isocurvature modes are expected to rule out significant non-gaussianity at higher orders as well - although a quantitative calculation is beyond the scope of this paper. Higher order non-gaussianity parameters are considered briefly in section 5.4.

5 Further consideration of constraints from isocurvature modes

In section 4, constraints were placed separately on f_{NL} and g_{NL} separately, assuming that DM was entirely composed of primordial black holes. In this section, the calculation is extended to account for more general models.

5.1 Isocurvature modes from f_{NL} and g_{NL}

The presence of non-zero non-gaussianity parameters has been shown to create significant isocurvature modes, which has led to very tight constraints on these parameters under the assumption that DM is composed entirely of PBHs. The calculation is now extended to account for non-zero f_{NL} and g_{NL} simultaneously - for example, it is possible that the effect of a large positive f_{NL} and large negative g_{NL} can cancel out, leaving a very small isocurvature mode.

Because the non-gaussianity parameters may now become quite large, the full numeric calculation for the PBH abundance is used to derive a value for the PBH bias b , for example by using equations (8) or (9) rather than the much simpler equation (10).

Figure 7 shows the values of g_{NL} that are permitted for different values of f_{NL} for PBHs of mass $M_{PBH} = 10^{25}g$. Whilst large values of f_{NL} and g_{NL} are allowed, there needs to be significant fine tuning to ensure that the resultant isocurvature modes are not excluded by the *Planck* results - g_{NL} needs to have the correct value to $\mathcal{O}(0.1\%)$. We note that there is some uncertainty in the value of g_{NL} required for a given f_{NL} due to the uncertainty in the formation threshold ζ_c - although this does not affect the conclusion that large non-gaussianity parameters are not allowed unless very very finely tuned. This conclusion is expected to remain true for higher-order terms [37].

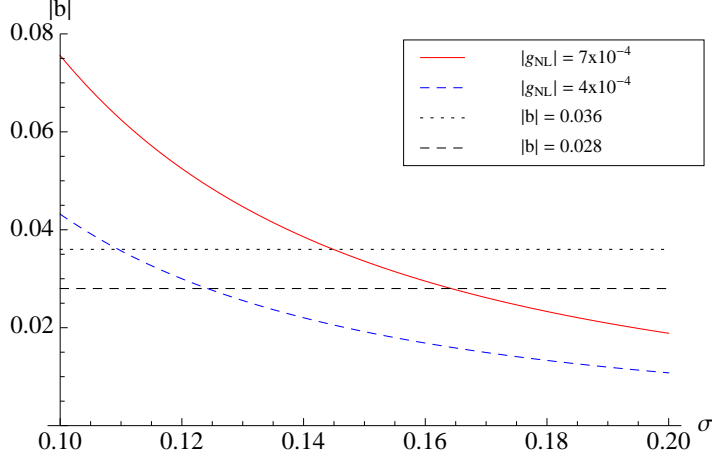


Figure 6: This plot shows the effects of a different σ on the PBH bias b arising from a g_{NL} term. A smaller value of σ suggests a larger bias factor. As the expression for b , equation (38), is anti-symmetric under a change of sign of g_{NL} , the results for negative and positive g_{NL} are shown on one plot - but with different constraints on the amplitude of $|b|$, represented by the dotted black lines. $|g_{NL}| = 7 \times 10^{-4}$ is typically excluded whilst $|g_{NL}| = 4 \times 10^{-4}$ is typically allowed. To generate these plots the value $\zeta_c = 1$ has been used. This range of σ is used because it is approximately the range of values required to generate the correct number of PBHs to form DM (assuming that perturbations are close to gaussian).

5.2 Fractional primordial black hole DM

So far, it has been assumed that DM is made entirely of PBHs. The calculation is now extended to account for the fact that PBHs may only make up a small fraction of DM, and this is parameterised by r_{PBH} , the ratio of PBH density to DM density.

$$r_{PBH} = \frac{\Omega_{PBH}}{\Omega_{DM}}. \quad (40)$$

In this case, the density of DM is described by

$$\Omega_{DM} = (1 + r_{PBH}b\zeta + 3\zeta)\bar{\Omega}_{DM}, \quad (41)$$

and the relative amplitude of the isocurvature modes is now given by $r_{PBH}b$. Therefore, from the *Planck* constraints on isocurvature modes instead give constraints on the factor $r_{PBH}b$,

$$-0.028 < r_{PBH}b < 0.036. \quad (42)$$

The constraints which can be placed on the non-gaussianity parameters therefore depend upon the PBH DM fraction, r_{PBH} . Figure 8 shows the allowed values of f_{NL} , g_{NL} and r_{PBH} if the PBH mass is $M_{PBH} = 10^{25}$ g.

- Large r_{PBH} : if PBHs make up a large fraction of DM then very tight constraints can be placed on the non-gaussianity parameters, f_{NL} , $g_{NL} < \mathcal{O}(10^{-2})$.
- Small r_{PBH} : if PBHs make up a small fraction of DM, $r_{PBH} < 0.1$, then the constraints on f_{NL} and g_{NL} weaken significantly. However, the non-gaussianity parameters only become larger than 1 if $r_{PBH} < \mathcal{O}(10^{-3})$. In the case where r_{PBH} is very small, the non-gaussianity

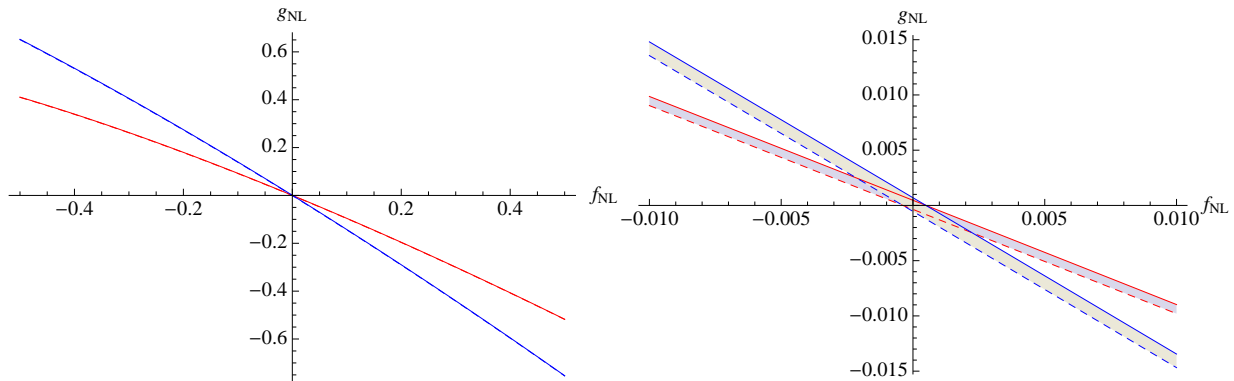


Figure 7: The constraints on simultaneous f_{NL} and g_{NL} are displayed. The right plot simply displays the central region of the plot on the left. The solid lines represent an upper limit from fully correlated isocurvature modes, whilst the dotted lines represent a lower limit from fully anti-correlated isocurvature modes. There is some uncertainty in the value of g_{NL} given a value of f_{NL} due to uncertainty in the critical value ζ_c - the blue lines are obtained using $\zeta_c = 0.8$, and the red lines are obtained using $\zeta_c = 1.2$. It can nonetheless be seen that large f_{NL} or g_{NL} are excluded unless very finely tuned. The shaded regions between the lines can be considered as 2σ contour plots from the *Planck* constraints.

parameters can become large and it is crucial to account for the effect of a non-gaussian distribution on the PBH forming scale, as done in this paper - as seen by the strong asymmetry for positive and negative f_{NL} .

As r_{PBH} becomes very small, f_{NL} can become large and positive, but is still strongly restricted to not be large and negative. This is partly due to the fine tuning of the small scale power spectrum necessary to produce a small but not too large number of PBHs when f_{NL} is negative - even a very small amount of modal coupling can mean that this fine tuning is disrupted in different regions of the universe, causing large amounts of variation in the number density of PBHs forming. This effect is not seen unless the non-gaussian distribution on small scales is accounted for. For g_{NL} , the constraints do not depend much on the sign of g_{NL} , and the small difference is due almost entirely to the difference in constraints from *Planck* on fully, or fully anti-, correlated modes.

5.3 Intermediate modes

The intermediate scales in between the large scales visible in the CMB and the small scale at which PBHs form have so far been ignored. This is a valid approximation if the power spectrum is small at all scales except for a narrow peak at the PBH forming scale, as in figure 2. However, this may not be the case if, for example, the power spectrum has a broad peak, as seen in figure 9, or becomes blue at small scales. In this case, the abundance of PBHs, as well as the amplitude of isocurvature modes, can be significantly affected by the presence of perturbations on these intermediate modes.

If the power spectrum of the intermediate modes is not small, they will have a significant effect on the number of PBHs that form, as well as the isocurvature modes visible in PBH DM. This will be investigated in a similar to the peak-background split, and the curvature perturbation is split into short, intermediate, and long components:

$$\zeta_G = \zeta_s + \zeta_i + \zeta_l. \quad (43)$$

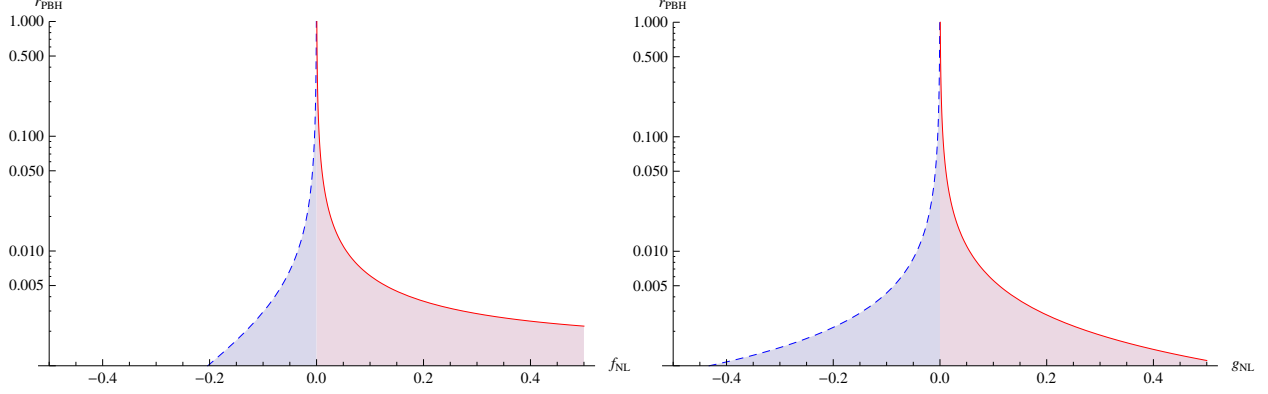


Figure 8: In the case where PBHs only make up a small fraction of the DM content of the universe, parameterised by r_{PBH} , the constraints on f_{NL} and g_{NL} can become significantly weaker. This is due to the fact a large isocurvature mode in the PBH density would only translate into a small isocurvature mode in the DM density. The plots above show the allowed values of f_{NL} and g_{NL} for different values of r_{PBH} . Whilst the plots show the constraints for PBHs of mass $M_{PBH} = 10^{25}$ g, the constraints are not very sensitive to the PBH mass.

The mass fraction of a given region of the universe going into PBHs is then calculated as before, as a function of ζ_i and ζ_l , in addition to f_{NL} , g_{NL} , σ_s and ζ_c ,

$$\beta = \beta(\zeta_i, \zeta_l). \quad (44)$$

However, the intermediate modes are too small scale to be observed in the CMB, and should therefore be averaged over:

$$\beta(\zeta_l) = \int_{-\infty}^{\infty} \tilde{\beta}(\zeta_i, \zeta_l) P(\zeta_i) d\zeta_i, \quad (45)$$

where $\tilde{\beta}$ is the value of β in different (intermediate-scale) regions of the universe, and $P(\zeta_i)$ is the probability density function of ζ_i , and is given by:

$$P(\zeta_i) = \frac{1}{\sqrt{2Pi\langle\zeta_i^2\rangle}} \exp\left(-\frac{\zeta_i^2}{2\langle\zeta_i^2\rangle}\right). \quad (46)$$

In principle, $\langle\zeta_i^2\rangle$, can be obtained by integrating the power spectrum over the relevant range of scales. However, since this is unknown and model dependant, it is parameterised here by r_{int} , the ratio of the variance of intermediate modes $\langle\zeta_i^2\rangle$ to the variance of the short modes σ_s^2

$$r_{int} = \frac{\langle\zeta_i^2\rangle}{\sigma_s^2}. \quad (47)$$

The value of $\langle\zeta_i^2\rangle$ can become larger than σ_s^2 due to the fact that many scales can contribute to ζ_i , but only one scale contributes to ζ_s . $\langle\zeta_i^2\rangle$ is calculated by integrating the power spectrum over the range of scales considered to be intermediate

$$\langle\zeta_i^2\rangle = \int_{k_{min}}^{k_{max}} \frac{dk}{k} \mathcal{P}_{\zeta}(k), \quad (48)$$

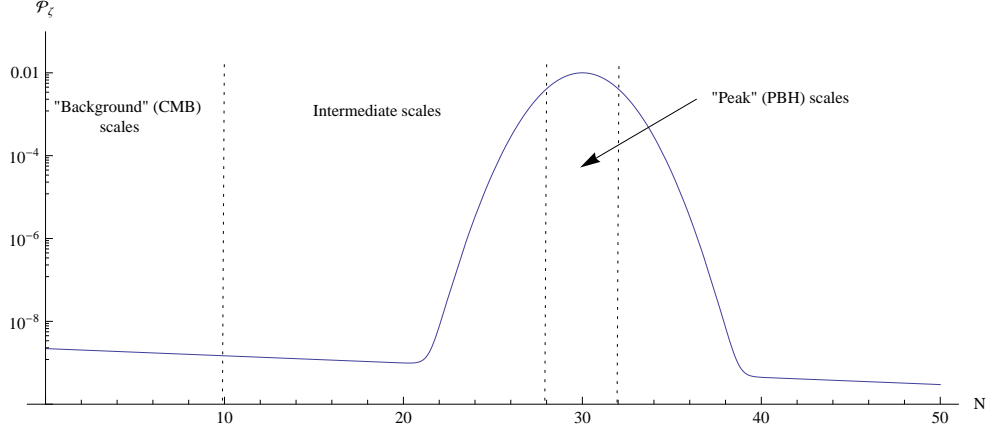


Figure 9: An example of a power spectrum containing a broad peak. In this paper, there are 3 difference scales: the large "background" scales visible in the CMB, the small "peak" PBH forming scale (the exact scale of which depends on the mass PBH being considered), and the intermediate scales between the background and the peak. In such a case, the intermediate modes can have an effect on the PBH bias.

and can become large if the power spectrum is large over a significant range of this integration. In contrast, the PBH scale perturbations ζ_s are only composed of perturbations from one scale⁶. Therefore, $\langle \zeta_i^2 \rangle$ can become significantly larger than σ_s^2 even though the power spectrum has its largest value at the PBH scale. However, it is likely that in such a scenario, PBHs of multiple mass scales would be produced, which is discussed later.

The amplitude of the isocurvature modes therefore depends on the non-gaussianity parameters, the small scale power spectrum σ_s^2 , the formation threshold ζ_c , and r_{int} . A value for the PBH bias b is then calculated numerically, figure 10 displays b dependant on these variables. The effect of intermediate modes on the amplitude of isocurvature modes is relatively small for small f_{NL} or g_{NL} unless the variance of the intermediate scales is very large. The constraints on f_{NL} can be weakened by a factor $\mathcal{O}(1)$, although the constraints on g_{NL} are not significantly affected.

Note that a model where the power spectrum is large over a broad range of scales would likely also produce PBHs with a large range of masses, and vice versa. This fact does not affect the conclusions presented here, as the production of PBHs at all mass scales would be affected by bias in a similar way. We have shown that intermediate modes can significantly affect the PBH bias, although which modes are considered to be intermediate depends on the scale at which PBHs are forming, and therefore on the mass of PBHs forming. The exact constraints depend on the form of the power spectrum, and must therefore be calculated on a model by model basis, which goes beyond the scope of this paper - although the constraints will not be weaker than $f_{NL}, g_{NL} \lesssim 10^{-3}$.

5.4 Higher Order terms

Whilst only the constraints on f_{NL} and g_{NL} have been calculated here, very tight constraints on higher order non-gaussianity parameters are also expected. In the same way that a g_{NL} term has a small but significant effect on f_{NL} , equation (5), higher order terms affect the previous term.

⁶Formally, σ_s^2 is given by integrating the power spectrum multiplied by a window function. However, provided that the spectral index is close to 1, or alternatively there is a peak spanning approximately 1 e-fold at the PBH scale, σ_s^2 is approximately equal to the power spectrum at that scale.

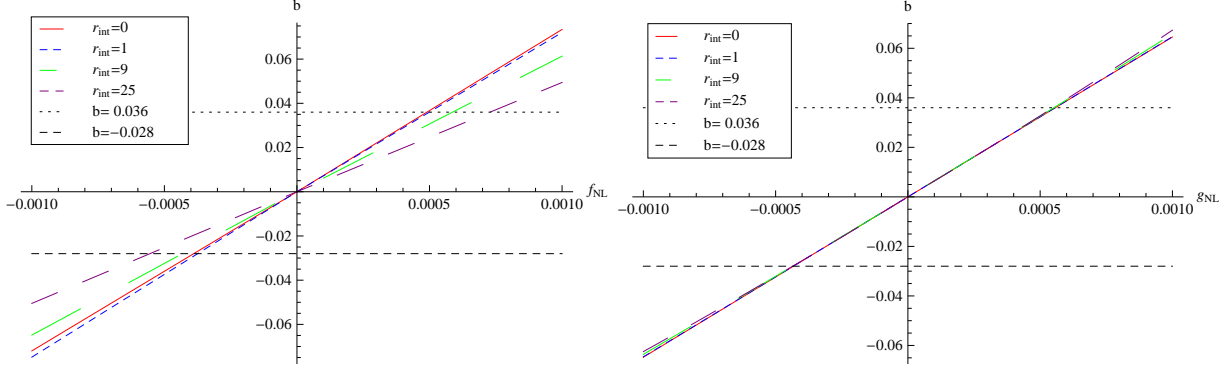


Figure 10: The effect of intermediate modes on the PBH bias b is displayed for $M_{PBH} = 10^{25}g$. The variance of the intermediate modes is parameterised by r_{int} , the ratio of $\langle \zeta_{int}^2 \rangle$ to σ_s^2 . The effect is negligible unless r_{int} becomes large, in which case the PBH bias arising from an f_{NL} term becomes significantly smaller, although has little effect for g_{NL} .

Because the mass fraction of the universe forming PBHs is extremely sensitive to non-gaussianity parameters at higher orders [37], even very small changes to higher order non-gaussianity parameters due to modal coupling creates significant perturbations in the PBH density at large scales. As an example, we will consider a 5th order term in local-type non-gaussianity:

$$\zeta = \zeta_G + \frac{81}{625} i_{NL} \zeta_G^5. \quad (49)$$

Utilising the peak-background split gives a 4th order term at small scales, \tilde{h}_{NL} , given by

$$\tilde{h}_{NL} = 3i_{NL}\zeta_l. \quad (50)$$

Inserting $\zeta_l \approx 10^{-5}$ and $i_{NL} = 10^{-3}$ gives $\tilde{h}_{NL} \approx 10^{-8}$. The modulation of the \tilde{h}_{NL} by the long wavelength mode ζ_l then generates a perturbation in the density of PBHs forming, $\delta_\beta \approx 10^{-6}$. In the picture of PBH DM, this results in a fully-correlated isocurvature mode, with a bias factor of $b \approx 0.1$ - which is excluded by Planck. Because it can be shown that high order terms have an effect on the preceding term which is linear in ζ , tight constraints are expected on such non-gaussianity parameters, only weakening slightly as higher order terms are considered.

6 Summary

The effect of modal coupling under the presence of non-gaussianity of the local type produces significant isocurvature modes in the density of PBHs in the early universe. If PBHs make up a significant fraction of DM, the constraints on isocurvature modes in cold DM from *Planck* can be used to constrain the non-gaussianity parameters - in this paper we have considered f_{NL} and g_{NL} . Using the constraints from *Planck* on isocurvature modes enables tight constraints to be placed on f_{NL} and g_{NL} ,

$$|f_{NL}|, |g_{NL}| < \mathcal{O}(10^{-3}), \quad (51)$$

unless f_{NL} and g_{NL} have opposite signs and have been extremely finely tuned so that the effect from each term cancels. Cases where the constraints could become weaker have also been considered: if the power spectrum is large on scales between those visible in the CMB and the PBH forming scale, or if DM is only partially composed of PBHs, finding that under these conditions the constraints

weaken very slightly (unless PBHs make up a very tiny fraction of DM). Therefore, the detection of significant numbers of PBHs would rule out significant local non-gaussianity, and vice versa. Our constraints are almost independent of the PBH mass, and can also be applied to Planck mass relics which may be left behind from the evaporation of small PBHs.

The production of isocurvature modes can therefore be used to constrain PBH forming models which may otherwise be permitted. For example, we will consider here two models which may be ruled out as mechanisms to produce PBH DM:

- Hybrid inflation: hybrid inflation typically predicts a non-zero f_{NL} , but there is some freedom in the exact value. [39] predicts $f_{NL} \approx -1/N_*$, where N_* is the number of e-folds between horizon exit of some pivot scale and the end of horizon. Inflation is believed to have lasted at least 50 – 60 e-folds, which would give $f_{NL} = \mathcal{O}(10^{-2})$ - several orders of magnitude higher than allowed by the constraints presented here. [40] predicts that f_{NL} can span a range of values from 10^{-2} to 10^5 - the entire range of which would be ruled out as a method of producing PBH DM.
- The curvaton: the amount of non-gaussianity in the curvaton model depends on the density parameter, Ω_χ , of the curvaton, χ , at the time it decays into radiation: $f_{NL} = -5/4$ if $\Omega_\chi = 1$ [41]. Although higher order local non-gaussianity terms are generated, it is unlikely that these will generate small isocurvature perturbations to evade the constraints.

There are, however, limitations to the calculations carried out in this paper. Notably, we have only considered local-type non-gaussianity, and throughout it has been assumed that f_{NL} and g_{NL} are scale invariant. We have also only calculated the dependence of isocurvature modes on f_{NL} and g_{NL} , and shown them to a roughly equivalent effect - with g_{NL} having only a marginally smaller effect. Higher order terms are therefore also likely to have a similar effect on isocurvature modes. We also note that it has recently been observed that sub-horizon perturbations at the time of PBH formation have an effect on whether a perturbation will collapse to form a PBH or not [42]. The expected amplitude of these sub-horizon modes would be affected by modal coupling - and therefore affect the amount of PBHs forming, affecting the isocurvature modes. However, this effect is expected to be negligible whilst the non-gaussianity parameters are very small.

7 Acknowledgements

SY is supported by an STFC studentship, and CB is supported by a Royal Society University Research Fellowship. We thank David Seery, John Miller, Yuichiro Tada and Shuichiro Yokoyama for useful discussions.

A Full expression for δ_β from a g_{NL} term

For completeness, the full expression for δ_β arising from a g_{NL} term is included - though this expression is still only valid for small g_{NL} . This expression would replace the simpler equation (38).

$$\begin{aligned}
\delta_\beta = & \left(-503^{1/3} 10^{2/3} + \left(-27\sqrt{g_{NL}\zeta_c} + \sqrt{300 + 729g_{NL}\zeta_c^2} \right)^{1/3} \left(45 \cdot 3^{2/3} 10^{1/3} \sqrt{g_{NL}\zeta_c} \right. \right. \\
& - 5 \cdot 3^{1/6} 10^{1/3} \sqrt{100 + 243g_{NL}\zeta_c^2} + 100 \left(-27\sqrt{g_{NL}\zeta_c} + \sqrt{300 + 729g_{NL}\zeta_c^2} \right)^{1/3} \\
& \left. \left. - 54g_{NL}\sigma^2 \left(-27\sqrt{g_{NL}\zeta_c} + \sqrt{300 + 729g_{NL}\zeta_c^2} \right)^{1/3} \right) \right) \left(-253^{1/3} 10^{2/3} \sqrt{g^3 (100 + 243g_{NL}\zeta_c^2)} \right. \\
& \left(-27\sqrt{g_{NL}\zeta_c} + \sqrt{300 + 729g_{NL}\zeta_c^2} \right)^{2/3} - 250\sqrt{3}g_{NL}^{3/2} \left(3^{1/6} 10^{1/3} \sqrt{100 + 243g_{NL}\zeta_c^2} - 20(-27\sqrt{g_{NL}\zeta_c} \right. \\
& \left. \left. + \sqrt{300 + 729g_{NL}\zeta_c^2} \right)^{1/3} \right) + 225g_{NL}^2\zeta_c \left(30 \cdot 3^{1/6} 10^{1/3} - 6\sqrt{100 + 243g_{NL}\zeta_c^2} (-27\sqrt{g_{NL}\zeta_c} \right. \\
& \left. \left. + \sqrt{300 + 729g_{NL}\zeta_c^2} \right)^{1/3} + 3^{5/6} 10^{2/3} \left(-27\sqrt{g_{NL}\zeta_c} + \sqrt{300 + 729g_{NL}\zeta_c^2} \right)^{2/3} \right) \\
& + 243 \cdot 3^{1/6} 10^{1/3} g_{NL}^3 \sigma^2 \zeta_c \left(30 + 10^{1/3} \left(-81\sqrt{g_{NL}\zeta_c} + 3\sqrt{300 + 729g_{NL}\zeta_c^2} \right)^{2/3} \right) \\
& - 27 \cdot 3^{1/3} g_{NL}^{5/2} \left(-4503^{1/6} \zeta_c^2 \left(-27\sqrt{g_{NL}\zeta_c} + \sqrt{300 + 729g_{NL}\zeta_c^2} \right)^{1/3} \right. \\
& \left. \left. + 10^{1/3} \sigma^2 \sqrt{100 + 243g_{NL}\zeta_c^2} \left(10 \cdot 3^{1/3} + 10^{1/3} \left(-27\sqrt{g_{NL}\zeta_c} + \sqrt{300 + 729g_{NL}\zeta_c^2} \right)^{2/3} \right) \right) \right) \\
& \left(150 \cdot 30^{1/3} \sigma^2 \sqrt{\frac{100}{g_{NL}}} + 243\zeta_c^2 \left(-27g_{NL}^2\zeta_c + \sqrt{3} \sqrt{g^3 (100 + 243g_{NL}\zeta_c^2)} \right)^{5/3} \left(-103^{1/3} \right. \right. \\
& \left. \left. + 10^{1/3} \left(-27\sqrt{g_{NL}\zeta_c} + \sqrt{300 + 729g_{NL}\zeta_c^2} \right)^{2/3} \right) \right)^{-1} \zeta.
\end{aligned}$$

B Comparison with “Primordial black holes as biased tracers”

In their paper, “Primordial black holes as biased tracers” [27], Tada and Yokoyama derive an expression for the *scale-dependant bias* given by

$$\Delta b(k) = 2f_{NL}\mathcal{M}_l^{-1}(k)\frac{\delta_c^2}{\sigma_s^2}. \quad (52)$$

This is equivalent to equation (34) in this paper. The factor of 3/5 difference is due to a different definition of f_{NL} , and the factor $\mathcal{M}_l^{-1}(k)$ is a result of their use of the density contrast rather than the curvature perturbation. The +1 in the brackets of equation (34) is a small correction and can be neglected. Therefore, the results for very small f_{NL} in the 2 papers are equivalent. In figure 11 the two expressions are compared. For $|f_{NL}| < \mathcal{O}(10^{-2})$ the two calculations match well, but diverge rapidly for larger $|f_{NL}|$.

It is therefore necessary to use the full calculation derived in this paper in situations where f_{NL} could become larger than 10^{-2} . Whilst such a large value of f_{NL} is generally excluded by the constraints on isocurvature modes in the PBH DM scenario, it is relevant where higher order terms are considered, or that PBHs form a sub-dominant component of DM.

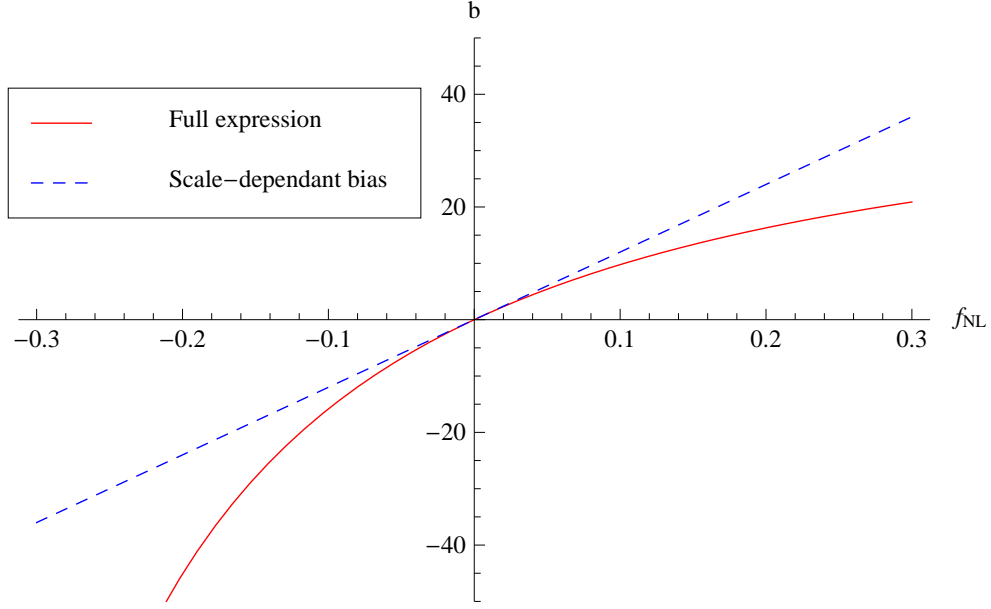


Figure 11: A comparison of the results derived in this paper with those derived in [27]. The solid red line denotes the full expression for the PBH bias given by equation (33), and the dashed blue line represent the *scale-dependant bias* given by equation (14) in [27]. To make these plots, the values $\sigma_s = 0.1$ and $\zeta_c = 1$ have been used.

References

- [1] B. Carr, K. Kohri, Y. Sendouda, and J. Yokoyama, *New cosmological constraints on primordial black holes*, *Phys.Rev.* **D81** (2010) 104019, [[arXiv:0912.5297](#)].
- [2] P. Pani and A. Loeb, *Exclusion of the remaining mass window for primordial black holes as the dominant constituent of dark matter*, [arXiv:1401.3025](#).
- [3] F. Capela, M. Pshirkov, and P. Tinyakov, *A comment on "Exclusion of the remaining mass window for primordial black holes ..."*, [arXiv:1402.4671](#).
- [4] G. Defillon, E. Granet, P. Tinyakov, and M. H. Tytgat, *Tidal capture of primordial black holes by neutron stars*, *Phys.Rev.* **D90** (2014), no. 10 103522, [[arXiv:1409.0469](#)].
- [5] B. J. Carr, J. Gilbert, and J. E. Lidsey, *Black hole relics and inflation: Limits on blue perturbation spectra*, *Phys.Rev.* **D50** (1994) 4853–4867, [[astro-ph/9405027](#)].
- [6] M. Drees and E. Erfani, *Running-Mass Inflation Model and Primordial Black Holes*, *JCAP* **1104** (2011) 005, [[arXiv:1102.2340](#)].
- [7] E. Bugaev and P. Klimai, *Axion inflation with gauge field production and primordial black holes*, [arXiv:1312.7435](#).
- [8] E. Bugaev and P. Klimai, *Formation of primordial black holes from non-Gaussian perturbations produced in a waterfall transition*, *Phys.Rev.* **D85** (2012) 103504, [[arXiv:1112.5601](#)].

- [9] D. H. Lyth, *The hybrid inflation waterfall and the primordial curvature perturbation*, *JCAP* **1205** (2012) 022, [[arXiv:1201.4312](#)].
- [10] I. F. Halpern, M. P. Hertzberg, M. A. Joss, and E. I. Sfakianakis, *A Density Spike on Astrophysical Scales from an N-Field Waterfall Transition*, [arXiv:1410.1878](#).
- [11] C.-M. Lin and K.-W. Ng, *Primordial Black Holes from Passive Density Fluctuations*, *Phys.Lett.* **B718** (2013) 1181–1185, [[arXiv:1206.1685](#)].
- [12] S. Hotchkiss, A. Mazumdar, and S. Nadathur, *Observable gravitational waves from inflation with small field excursions*, *JCAP* **1202** (2012) 008, [[arXiv:1110.5389](#)].
- [13] A. Linde, S. Mooij, and E. Pajer, *Gauge field production in supergravity inflation: Local non-Gaussianity and primordial black holes*, *Phys.Rev.* **D87** (2013), no. 10 103506, [[arXiv:1212.1693](#)].
- [14] E. Torres-Lomas, J. C. Hidalgo, K. A. Malik, and L. A. Urea-Lpez, *Formation of subhorizon black holes from preheating*, *Phys.Rev.* **D89** (2014) 083008, [[arXiv:1401.6960](#)].
- [15] T. Suyama, Y.-P. Wu, and J. Yokoyama, *Primordial black holes from temporally enhanced curvature perturbation*, *Phys.Rev.* **D90** (2014) 043514, [[arXiv:1406.0249](#)].
- [16] A. M. Green, *Primordial Black Holes: sirens of the early Universe*, [arXiv:1403.1198](#).
- [17] K. Jedamzik and J. C. Niemeyer, *Primordial black hole formation during first order phase transitions*, *Phys.Rev.* **D59** (1999) 124014, [[astro-ph/9901293](#)].
- [18] A. M. Green and A. R. Liddle, *Constraints on the density perturbation spectrum from primordial black holes*, *Phys.Rev.* **D56** (1997) 6166–6174, [[astro-ph/9704251](#)].
- [19] A. S. Josan, A. M. Green, and K. A. Malik, *Generalised constraints on the curvature perturbation from primordial black holes*, *Phys.Rev.* **D79** (2009) 103520, [[arXiv:0903.3184](#)].
- [20] S. Shandera, A. L. Erickcek, P. Scott, and J. Y. Galarza, *Number Counts and Non-Gaussianity*, *Phys.Rev.* **D88** (2013) 103506, [[arXiv:1211.7361](#)].
- [21] **Planck Collaboration** Collaboration, P. Ade *et. al.*, *Planck 2015. XX. Constraints on inflation*, [arXiv:1502.0211](#).
- [22] D. Wands, N. Bartolo, S. Matarrese, and A. Riotto, *An Observational test of two-field inflation*, *Phys.Rev.* **D66** (2002) 043520, [[astro-ph/0205253](#)].
- [23] S. Young and C. T. Byrnes, *The long-short wavelength mode coupling tightens primordial black hole constraints*, [arXiv:1411.4620](#).
- [24] J. M. Maldacena, *Non-Gaussian features of primordial fluctuations in single field inflationary models*, *JHEP* **0305** (2003) 013, [[astro-ph/0210603](#)].
- [25] E. Pajer, F. Schmidt, and M. Zaldarriaga, *The Observed Squeezed Limit of Cosmological Three-Point Functions*, *Phys.Rev.* **D88** (2013), no. 8 083502, [[arXiv:1305.0824](#)].
- [26] T. Tanaka and Y. Urakawa, *Dominance of gauge artifact in the consistency relation for the primordial bispectrum*, *JCAP* **1105** (2011) 014, [[arXiv:1103.1251](#)].

- [27] Y. Tada and S. Yokoyama, *Primordial black holes as biased tracers*, [arXiv:1502.0112](#).
- [28] J. C. Niemeyer and K. Jedamzik, *Dynamics of primordial black hole formation*, *Phys.Rev.* **D59** (1999) 124013, [[astro-ph/9901292](#)].
- [29] I. Hawke and J. Stewart, *The dynamics of primordial black hole formation*, *Class.Quant.Grav.* **19** (2002) 3687–3707.
- [30] I. Musco, J. C. Miller, and L. Rezzolla, *Computations of primordial black hole formation*, *Class.Quant.Grav.* **22** (2005) 1405–1424, [[gr-qc/0412063](#)].
- [31] I. Musco, J. C. Miller, and A. G. Polnarev, *Primordial black hole formation in the radiative era: Investigation of the critical nature of the collapse*, *Class.Quant.Grav.* **26** (2009) 235001, [[arXiv:0811.1452](#)].
- [32] T. Harada, C.-M. Yoo, and K. Kohri, *Threshold of primordial black hole formation*, *Phys.Rev.* **D88** (2013), no. 8 084051, [[arXiv:1309.4201](#)].
- [33] T. Nakama, T. Harada, A. Polnarev, and J. Yokoyama, *Identifying the most crucial parameters of the initial curvature profile for primordial black hole formation*, [arXiv:1310.3007](#).
- [34] M. Shibata and M. Sasaki, *Black hole formation in the Friedmann universe: Formulation and computation in numerical relativity*, *Phys.Rev.* **D60** (1999) 084002, [[gr-qc/9905064](#)].
- [35] S. Young, C. T. Byrnes, and M. Sasaki, *Calculating the mass fraction of primordial black holes*, *JCAP* **1407** (2014) 045, [[arXiv:1405.7023](#)].
- [36] C. T. Byrnes, E. J. Copeland, and A. M. Green, *Primordial black holes as a tool for constraining non-Gaussianity*, *Phys.Rev.* **D86** (2012) 043512, [[arXiv:1206.4188](#)].
- [37] S. Young and C. T. Byrnes, *Primordial black holes in non-Gaussian regimes*, *JCAP* **1308** (2013) 052, [[arXiv:1307.4995](#)].
- [38] C. T. Byrnes, K. Koyama, M. Sasaki, and D. Wands, *Diagrammatic approach to non-Gaussianity from inflation*, *JCAP* **0711** (2007) 027, [[arXiv:0705.4096](#)].
- [39] S. Clesse, B. Garbrecht, and Y. Zhu, *Non-Gaussianities and Curvature Perturbations from Hybrid Inflation*, *Phys.Rev.* **D89** (2014), no. 6 063519, [[arXiv:1304.7042](#)].
- [40] D. Mulryne, S. Orani, and A. Rajantie, *Non-Gaussianity from the hybrid potential*, *Phys.Rev.* **D84** (2011) 123527, [[arXiv:1107.4739](#)].
- [41] M. Sasaki, J. Valiviita, and D. Wands, *Non-Gaussianity of the primordial perturbation in the curvaton model*, *Phys.Rev.* **D74** (2006) 103003, [[astro-ph/0607627](#)].
- [42] T. Nakama, *The double formation of primordial black holes*, *JCAP* **1410** (2014), no. 10 040, [[arXiv:1408.0955](#)].

$a(t)$

Late time comoving slicing

Uniform CDM density slicing after PBH formation

Uniform radiation density slicing

Initial uniform density slicing

x

